



Chiang Mai J. Sci. 2018; 45(4) : 1796-1810

<http://epg.science.cmu.ac.th/ejournal/>

Contributed Paper

Characterization of Crystalline Structure and Thermostability of Debranched Chickpea Starch-Lauric Acid Complexes Prepared Under Different Complexation Conditions

Suchitra Wongprayoon [a], Thierry Tran [b,c], Olivier Gibert [c], Eric Dubreucq [d], Kuakoon Piyachomkwan [e] and Klanarong Sriroth* [a]

[a] Department of Biotechnology, Faculty of Agro-Industry, Kasetsart University, Bangkok 10900, Thailand.

[b] CIAT/CIRAD, UMR Qualisud, CGIAR Research Program on Roots, Tubers and Bananas (RTB), CIAT, KM 17 Recta Cali-Palmira, Cali, Colombia.

[c] CIRAD, UMR Qualisud, TAB-95/16, 73 Rue JF Breton, 34398 Montpellier, France.

[d] Montpellier SupAgro, UMR IATE, 2 Place Viala, 34060 Montpellier, France.

[e] Cassava and Starch Technology Research Unit, National Center for Genetic Engineering and Biotechnology, Pathumthani 12120, Thailand.

* Author for correspondence; e-mail: aapkrs@ku.ac.th

Received: 22 December 2017

Accepted: 5 January 2018

ABSTRACT

Chickpea starch was debranched with pullulanase, then complexed with lauric acid (LA) using two starch concentrations (3 and 10% w/w), two starch/LA mole ratios (1:0.1 and 1:1 mol anhydroglucose unit/mol LA) and two complexation temperatures (60 and 95°C). Different conditions influenced the formation, crystalline structure, morphology and thermostability of the complexes. Complexation occurred under the same conditions, and in competition with, retrogradation. Lower starch concentration favored the formation of complexes. At 3% starch concentration, complexation at 60°C produced more complexes, but with lower thermostability (T_p 96°C) and smaller crystallite sizes (4.78-4.83 nm), compared to complexes obtained at 95°C (111-117°C, 13.18-14.31 nm) that exhibited a highly crystalline torus/disc spherulitic morphology. These results confirm that the properties of starch-fatty acid complexes can be tailored to meet specific application requirements, by adjusting both the completed debranching and complexation conditions.

Keywords: helical inclusion complex, debranched chickpea starch, lauric acid, complexation conditions

1. INTRODUCTION

Starch inclusion complexes are a non-covalent interaction between primarily the amylose component of starch and various hydrophobic compounds. Their key

properties, in particular a single left-handed helix structure with a hydrophobic internal cavity and a hydrophilic outside surface [1] and high melting temperature make them

attractive for nanoencapsulation of compounds that are insoluble in water or sensitive to oxygen, light or thermal stress such as volatile flavor/aroma compounds, bioactive substances, nutrients and nutraceuticals [2-3]. Complexation by amylose increases the stability, solubility, dispersibility, bioavailability and controlled release properties of the encapsulated compounds. Starch inclusion complexes are less sensitive to enzyme hydrolysis than non-complexed starch during digestion, which may be useful for low glycemic index diets, for instance as part of treatments for diabetics and obese patients [4]. In terms of sensory perception, the increase in paste viscosity and non-gelling properties of starch-fatty acid complexes can improve mouthfeel in low-fat food products [5]. For breadmaking, complex formation reduces the availability of starch molecules for retrogradation, which can reduce staling and increase the shelf-life of bread.

The formation, arrangement and structure at the molecular, nanometric and microscopic levels, the physicochemical properties and the yield of starch inclusion complexes are all affected by the method of preparation and complexing factors such as starch type and concentration, amylose content and degree of polymerization, complexing ligand structure and concentration, complexation temperature and time, pH, cooling rate, stirring during cooling, crystallization temperature and time, washing agent and cycle, and drying method [6-10].

To increase complex formation, the amylopectin component (typically 70-80% of starch) can be debranched using pullulanase or isoamylase enzymes, so as to release linear glucan chains able to participate in the complexation reaction. This method is considered more practical for mass

production of starch inclusion complexes compared to using purified amylose, which is more costly and more difficult to disperse in water and to cook. Previous works on starch debranching for inclusion complex formation investigated the effect of debranching conditions and time on the structure and digestibility of high amylose maize starch-fatty acid complexes [11], and the effect of fatty acid chain lengths and pH on the ability to form complexes of debranched waxy rice starch [12]. The effect of other factors on complex formation and properties has, to our knowledge, been less investigated.

For this study, chickpea starch was debranched and complexed with lauric acid (LA) which was used as a model compound. It has been reported that several medium- and long-chain fatty acids have a virucidal and bactericidal activity [13]. The complexes were produced by pullulanase debranching of gelatinized chickpea starch, and complexing of the resulting linear glucans and amylose mixtures with LA. The objective of the study was to investigate the effect of the complexation conditions including starch concentration, starch/LA mole ratio and complexation temperature on the formation, crystalline structure, morphology and thermostability of debranched chickpea starch-LA complexes.

2. MATERIALS AND METHODS

2.1 Materials

Chickpea seeds were purchased from Gravity Intertrade Co., Ltd. (Bangkok, Thailand). Pullulanase (EC 3.2.1.41) "Amano" 3 was obtained from Amano Enzyme Inc. (Nagoya, Japan) and had the pullulanase activity of 3.21×10^3 U/mL at pH 6.0 and 50°C. Food grade lauric acid (C12:0, purity $\geq 98\%$) was purchased from Sigma-Aldrich (M) Sdn. Bhd. (Kuala Lumpur, Malaysia).

All other chemicals used were of analytical reagent grade.

2.2 Isolation of Chickpea Starch

Chickpea starch was extracted by wet-milling the steeped split chickpeas (2:1 water-to-chickpea weight ratio), screening through a 170-mesh sieve, sedimenting for 2 h, rewashing and re-sedimenting three times, and drying at 50°C overnight. Dried starch was ground and screened through a 100-mesh sieve. The chickpea starch contained 33.4% amylose, as determined by the differential scanning calorimetric method based on the measurement of the melting enthalpy of the complex between amylose and L- α -lysophosphatidylcholine.

2.3 Debranching of Starch and Preparation of Debranched Chickpea Starch-LA Complexes

The effect of reaction conditions on the complexation of debranched chickpea starch and LA was systematically explored with (1) two levels of starch concentrations (3 and 10% w/w); (2) two starch/LA mole ratios (1:0.1 and 1:1 mol anhydroglucose unit (AGU)/mol LA) and (3) two complexation temperatures (60 and 95°C).

Chickpea starch (60 g, dry basis, db) was dispersed in distilled water to prepare slurries at 3% and 10% (w/w) starch concentrations. The slurries were adjusted to pH 6 with a hydrochloric acid solution (0.4 M) to optimize pullulanase reaction conditions, then cooked in a boiling water bath with stirring for 30 min. The pastes were cooled down to 50°C. The debranching reaction was started by adding pullulanase (45 U/g starch, db) and incubating at 50°C with stirring for 24 h. The enzyme reaction was terminated by boiling for 30 min.

The dispersions of gelatinized and debranched chickpea starch were cooled

from 100°C to the complexation temperatures of 60°C or 95°C. The LA was melted beforehand at 50°C, then added to the dispersions of chickpea starch (7.42 g and 74.2 g of pure LA for 1:0.1 and 1:1 starch/LA mole ratios, respectively). The dispersions were held at the determined temperatures for an additional 1 h with stirring. The mixtures were then left to slowly cool down without stirring for 24 h in a water bath (final temperature 38°C). The complexed starch was recovered by centrifugation (17,000 g, 15 min), washed three times with 50% ethanol/water mixture (v/v) and re-centrifuged to remove residues of uncomplexed LA. The wet precipitates were then immediately frozen with liquid nitrogen and subsequently freeze-dried. All freeze-dried samples were ground and screened through an 80-mesh sieve.

In order to verify that the debranching reaction was complete, the pullulanase-debranched chickpea starch samples were hydrolyzed with β -amylase according to the procedure of Hood and Mercier [14], and the β -amylolysis products were analyzed by high-performance anion-exchange chromatography with pulsed amperometric detection (HPAEC-PAD) (Dionex ICS-5000, Sunnyvale, CA, USA). All samples showed only two peaks at 3.1 and 4.5 minutes elution time, corresponding to maltose and maltotriose respectively, which confirmed the absence of branched fragments.

The effect of the pullulanase treatment was studied on whole starch through the release of shorter chains from amylopectin branches. For an amylose-containing starch, the debranching enzyme treatment should release a large proportion of shorter and a small proportion of longer linear chains from amylopectin, and a smaller proportion of longer linear chains from amylose [15]. The debranching of chickpea starch was

thus studied by HPAEC-PAD, following the procedure of Bertoft [16]. The chain length distribution of pullulanase-debranched chickpea starch is presented in Table 1.

Table 1. Chain length distribution of pullulanase-debranched chickpea starch.

Sample	% Chain length distribution			
	DP 6-12	DP 13-24	DP 25-36	DP \geq 37
Pullulanase-debranched chickpea starch	39	46	11	4

DP means degree of polymerization.

2.4 Wide Angle X-ray Diffraction (WAXD)

As X-ray diffraction intensity is affected by starch moisture content (MC), freeze-dried samples were conditioned over a saturated NaCl solution (a_w 0.75) for two weeks at 25°C (final MC 10.9% \pm 0.8). WAXD analysis was performed on a Bruker D8 Advance diffractometer using Cu K α_1 radiation (wavelength of 0.15406 nm) generated at 40 kV and 40 mA. The samples were scanned over the diffraction angle (2θ) range from 4° to 36° with a step size of 0.02° and a collection time of 1 s per step. Relative crystallinity (RC) was calculated as the percentage ratio of crystalline peak area to total diffraction area of the X-ray diffractogram.

In case of mixed crystal formation, a deconvolution method according to the method reported by Lopez-Rubio et al. [17] with modifications was performed to quantify the RC of the individual crystalline peaks and the percentage proportions of A, B, C or V-type polymorphs in total polymorphs by using MDI Jade 6.0 software (Materials Data Inc., Livermore, CA) following these steps: (i) diffractogram was smoothed with Savitzky-Golay algorithm and baseline-corrected by drawing a tangent baseline between 2θ at 4° to 36°; (ii) the smoothed curve was further baseline-corrected with the amorphous-minima baseline fitting and the resulting pattern represented the crystalline fraction; (iii) the

crystalline fraction pattern was modeled with Pearson VII function until a best fit was obtained; (iv) the fitting peaks were determined as the contribution of A, B, C or V-type polymorphs according to the actual peak position to the respective standard peak; and (v) the RC apportioned to each peak was calculated as the ratio of the individual peak crystalline area to the total crystalline area. The proportions of A, B, C and V-type polymorphs were calculated as the sums of the RC of the peaks contributing to each polymorph. The crystal size of complexes was estimated from the broadening of the peak at $2\theta = 7.5^\circ$, 13° and 20° which correspond to the planes (110), (130) and (310) of the V_{61} orthorhombic unit cell, respectively, using the Scherrer's equation: $D_{hkl} = 0.9\lambda/\beta\cos\theta$, where D_{hkl} is the crystal size, λ is the wave length of the X-ray used, β is the full width at half maximum and θ is the Bragg angle [18].

2.5 Scanning Electron Microscopy (SEM)

Scanning electron micrographs of the freeze-dried samples were obtained with a scanning electron microscope (FEI Quanta 450, FEI company, Netherlands). The powdered samples were sprinkled on double-sided adhesive tape attached to a circular specimen stub and were then sputter coated with gold. The samples were imaged at 5,000x magnification.

2.6 Quantification of Complexed LA by Gas Chromatography with Flame Ionization Detector (GC/FID)

The quantity of LA complexed with debranched chickpea starch was determined by the modified Weibull-Stoldt method. The sample (1 g, db) was suspended in 11.1% HCl (25 mL) and boiled gently with stirring for 40 min. The mixture was filtered and washed with warm distilled water until the filtrate was neutral. The filter paper with the residue was oven dried at 50°C overnight and transferred to a defatting extraction thimble followed by soxhlet extraction with chloroform-methanol (2:1, v/v) for 5 h. The remaining solvent was evaporated at 60°C. The extracted LA was solubilized in hexane (1 mL) for derivatization by silylation. The LA-hexane solution (200 µL) was transferred to a glass vial and 25 µL of each pyridine and MSTFA (N-Methyl-N-Trimethylsilyl-Trifluoroacetamide) were added. The vial was sealed and placed in a water bath at 50°C for 20 min. The LA trimethylsilyl ester was injected into a gas chromatographer (GC-2010 Plus, Shimadzu, Kyoto, Japan) equipped with a DB-5ht capillary column (15 m × 0.25 mm I.D., film thickness 0.1 mm, J&W P/N 122-5711, Agilent technologies Inc., Santa Clara, CA, USA) with a flame ionization detector (FID). Control, processing and data acquisition were performed with the Shimadzu LabSolutions software (Kyoto, Japan). The injector and detector temperatures were 280°C and 290°C, respectively. The oven temperature was equilibrated at 180°C, ramped up to 210°C at 25°C/min and kept constant for 5.2 min. The quantity of extracted LA was determined from a standard curve prepared with a series of LA trimethylsilyl ester solutions.

2.7 Differential Scanning Calorimetry (DSC)

The thermal properties of debranched chickpea starch-LA complexes were determined in triplicate with a differential scanning calorimeter (DSC 7, Perkin-Elmer, Norwalk, CT, USA). The freeze-dried samples (9 mg, db) were mixed with distilled water (21 mg), sealed in air-tight stainless steel pans and equilibrated overnight at ambient temperature. The samples were scanned from 20°C to 160°C at 10°C/min. An empty pan was used as a reference and indium was used to calibrate the DSC instrument. The onset (T_o), peak (T_p) and conclusion temperature (T_c), and enthalpy (ΔH , J/g dry starch) of the melting of the complexes were calculated with the Pyris data analysis software.

2.8 Statistical Analysis

Statistical analyses were performed using SPSS software. Statistical significance was evaluated at $p < 0.05$ level. Duncan's multiple range test was applied for comparison.

3. RESULTS AND DISCUSSION

3.1 Effect of Complexation Conditions on Complex Formation and Crystalline Structure

The formation of complexes between debranched chickpea starch and LA was confirmed by the presence of V-type WAXD patterns in all samples (Figure 1). The V-type pattern is characterized by three main peaks at diffraction angles $2\theta = 7.5^\circ$, 13° and 19.9° , and indicates the presence of V-hydrate (V_h), also called V_{ol} -type, left-handed, single-helices of unbranched glucan chains, consisting of six anhydroglucose units per helical turn, in the center of which complexing agents such as LA are entrapped [19]. These helices

are aggregated in crystalline clusters, with unit cell dimensions: $a = 1.36\text{--}1.37$ nm; $b = 2.37\text{--}2.58$ nm; $c = 0.78\text{--}0.81$ nm [2, 20]. Additionally, no diffraction peaks indicative

of free LA (sharp peaks at $2\theta = 6.5^\circ, 9.7^\circ, 16.2^\circ, 20.1^\circ, 21.4^\circ$ and 23.8°) was observed, which confirmed that all free LA was washed out during sample preparation.

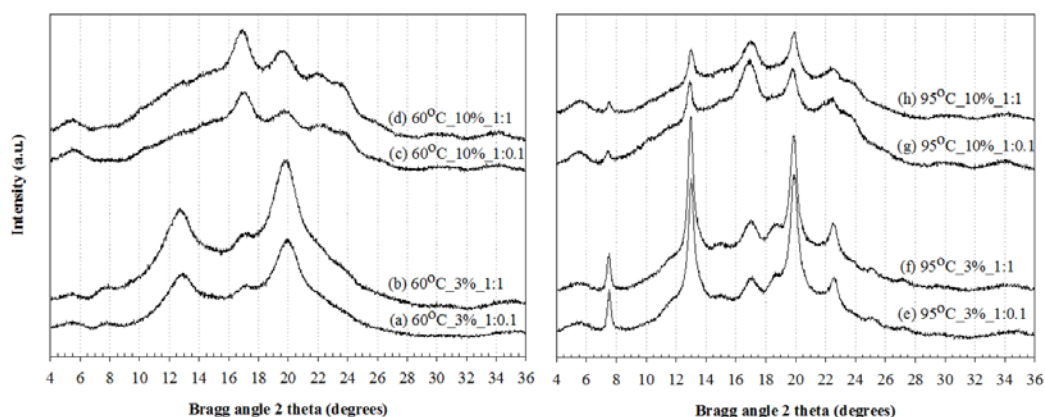


Figure 1. X-ray diffraction patterns of debranched chickpea starch-LA complexes prepared under different conditions: two complexation temperatures (60 and 95°C), two starch concentrations (3 and 10% w/w) and two starch/LA mole ratios (1:0.1 and 1:1 mol anhydroglucose unit/mol LA).

In addition to the V_{61} -type pattern, the diffractograms also showed diffraction peaks at $2\theta = 5.6^\circ, 17^\circ, 22^\circ$ and 24° which corresponded to a B-type crystalline polymorph indicative of starch retrogradation. The B-type crystallites were present in all samples, except those prepared at 95°C both 3% and 10% starch concentrations, which displayed the retrogradation of C- and C_b -type crystallites with a mixture of the A-type allomorph at $2\theta = 15^\circ$ and B-type allomorph at $2\theta = 5.6^\circ$ and 17° , or $2\theta = 5.6^\circ, 17^\circ$ and 24° for 3% and 10% starch solids, respectively. Additional tests of starch-lipid complexation indicated that retrogradation of starch, in particular of debranched fragments with lower molecular weights, was unavoidable, since it occurred under the same conditions as, and in competition with, lipids complexation. The type of polymorph and properties of crystallized debranched starch are dependent on the chain length

distribution and the crystallization conditions such as solids content, temperature and time. Low concentration, low temperature and long chains are known to induce B-type crystallization, whereas high concentration, high temperature and short chains favor the formation of A-type structure [21]. However, the occurrence of C- and C_b -type crystallites regardless of the starch concentration tested could be attributed to the co-influence of the high temperature crystallization and the chain length distribution of pea starch which contained intermediate chain length distributions between short and long chains, including the presence of longer chains from amylose fraction. Complexation at 95°C also showed two additional shoulder-shaped peaks at $2\theta = 11.6^\circ$ and 18.7° when starch concentration was low (3%), and showed an additional peak at $2\theta = 22.5^\circ$ whatever starch concentrations and starch/LA mole ratios. The additional peaks were similar to the peaks

in the V_{61} patterns observed for torus/disc-shaped spherulites formed from slowly-cooled dispersion of jet cooked cornstarch in the presence of the native lipid, and defatted cornstarch with palmitic acid [8], in which the intensity of shoulders tended to increase when the torus/disc spherulites were large and aggregated [9]. Similar patterns were also reported by Biais et al. [6] when preparing potato amylose-decanoic acid complex, Godet et al. [10] when complexing different amylose chain lengths with three fatty acid and Kim and Lim [22] when preparing nano-sized starch particles by hydrolyzing crude high amylose cornstarch-n-butanol complex with α -amylase. Two of these studies [6, 22] attributed the peak at $2\theta = 22.5^\circ$ to V-amylose polymorphism, whereas the shoulders at $2\theta = 11.6^\circ$ and 18.7° were not analyzed. Accordingly in the present study four diffractions at $2\theta = 7.5^\circ$, 13° , 19.9° and 22.5° were used as peaks representative of V_{61} -type complexes at 95°C , and the shoulders at $2\theta = 11.6^\circ$ and 18.7° were not taken into account.

Debranched chickpea starch and LA formed more complexes at lower starch concentration (3%), at both 60°C and 95°C complexation temperatures with the percentage proportion of V_{61} -type crystallites of 90-94% and 78-79%, respectively, depending on starch/LA mole ratios (Table 2). At higher starch concentration (10%), the complex formation dropped to 21-27% and 47-51% of V_{61} -type crystallites at 60°C and 95°C , respectively, depending on starch/LA mole ratios. A possible explanation is that the smaller average distance between debranched starch-LA complexes molecules at 10% starch solids favored the retrogradation reaction over the complexation reaction. The extent of retrogradation (Table 4) tends to confirm this interpretation.

The relative crystallinity (RC, %) attributable to V_{61} -type complexes was higher at 95°C than at 60°C , whereas the proportion of V_{61} -type crystallites was lower at 95°C , particularly at 3% starch concentration (Table 2), which again was related to the competition with the retrogradation reaction. Hoover and Ratnayake [23] attribute differences in RC to: (1) crystal size, (2) amount of crystalline regions, (3) the orientation of helices within the crystalline domains and (4) extent of interaction between helices. For these reasons, the discrepancy between the higher RC and the lower proportion of V_{61} -type crystallites formed at 95°C and 3% starch concentration could be explained by the higher formation rate of C-type crystallites. The crystal size of complexes increased at the higher complexation temperature (95°C) at both starch concentrations and both starch/LA mole ratios, as indicated by the narrower diffraction peaks (according to the equation of Scherrer, section 2.4). In contrast, the peaks corresponding to the V_{61} -type complexes formed at 60°C were broader than those formed at 95°C , indicating smaller sizes and a more heterogeneous size distribution of the crystallites. A possible explanation is that the higher temperature (95°C) was less favorable to nucleation, but enabled the crystals that formed grow (propagate) better and reach larger sizes. Schematic diagram of the mechanism for the formation of debranched starch complex as influenced by complexation temperature are shown in Figure 2.

The starch/LA mole ratio had a limited influence on the quantities of V_{61} -type crystallites formed. Adding more LA to the starch tended to increase the proportion of V_{61} -type crystallites; however, did not result in significant changes in the complex formation, indicating that maximum

complexation achievable under the different conditions tested was reached even at the lower LA concentration (1:0.1 starch/LA mole ratio). Tang and Copeland [24] reported that maximum complex formation occurred at different concentrations for each lipid, and was related to water solubility and critical micellar concentration of the lipid, due to the tendency of some lipids to self

associate in preference to forming starch-lipid complexes. The RC corresponding to V_{61} -type complexes increased with LA concentration at 10% starch, and decreased at 3% starch concentration. This may be related to interferences of free LA molecules, reducing the ability of single complex helices to pack into crystalline clusters [3].

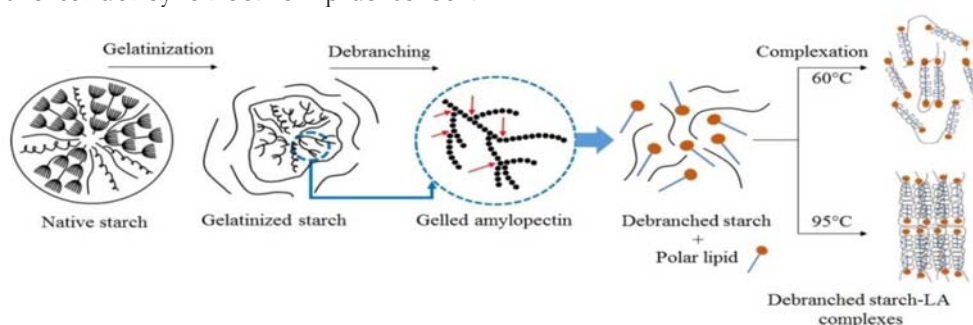


Figure 2. Schematic diagram of the mechanism for the formation of debranched starch-LA complexes as influenced by complexation temperature.

3.2 Content of LA in Debranched Chickpea Starch Complexes

The amounts of LA complexed with debranched chickpea starch (Table 3) were positively correlated with the proportion of V_{61} -type crystallites ($R^2 = 0.93$). The increase in starch concentration to 10% decreased the amounts of complexed LA to 0.20-0.22 g and 0.34-0.40 g/100 g dry samples at 60°C and 95°C, respectively. At 3% starch concentration, complexation at 60°C provided the highest amount of complexed LA. The starch/LA mole ratio had a limited influence on the amount of the complexed LA which was expected since the quantities of LA used in this study were large enough to form single helices of complexes with all available starch molecules under the different conditions tested even at lower LA concentration. However, increasing the LA concentration at 3% starch solids and 95°C reduced the amount of complexed LA, which could be due to a disruptive effect of

the concentration of LA: Le Bail et al. [25] mention that fatty acids at high concentrations can be trapped in polymer chains without forming a complex, which may reduce the availability of debranched starch to form inclusion complexes. This mechanism may also leave more debranched starch available for retrogradation, as evidenced by a slight increase in C-type crystallites from 10% to 13% (Table 2).

3.3 Morphology of Complexes by Scanning Electron Microscopy (SEM)

Regardless of starch/LA mole ratio, smaller crystallite complexes formed at 3% starch concentration and 60°C, and exhibited large irregularly shaped aggregate particles with cauliflower-like surface and size heterogeneity (20-40 μm) (Figure 3a, 3b). At 10% starch concentration under the same conditions, the morphology of complexes changed to mixtures of large coarse particles (15-30 μm) and dense

aggregates of irregularly shaped particles (Figure 3c, 3d). At 3% and 10% starch concentrations and 95°C, the crystallite complexes exhibited torus/disc-shaped spherulites ($\sim 10\ \mu\text{m}$). The majority of these were separate from others, while a smaller proportion formed clumps, which included non-spherulitic particles (Figure 3e, 3f, 3g, 3h). At 10% starch concentration and 95°C, the torus/disc spherulites were accompanied by large coarse particles, with the spherulites mostly located on the surface of the coarse particles (Figure 3g, 3h). Some micrographs suggested that some spherulites grew from the surfaces of the coarse particles. No obvious morphological changes of complexes were observed when the starch/LA mole ratio changed from 1:0.1 to 1:1. These results suggested that the difference in morphology of complexes (spherulites versus coarse particles) depended mainly on the complexation temperature, while the

proportion of spherulites depended on the starch concentration. Several studies reported that such spherulites form when the amylose inclusion complexes are laterally stacked by up and down folding into a lamellae structure, growing in a radial direction from a central nucleus. Additionally, imperfect stacking of individual lamellae and branching of lamellae during spherulite growth influenced spherulite morphology [26]. The formation of spherulites from native starch usually requires temperatures above 140°C, followed by slow cooling [9]. These high temperatures are necessary to destructure the starch granules before spherulites can form. In the present study starch granules were destructured during the debranching treatment, which enabled the formation of torus/disc spherulites at a markedly lower temperature (95°C), from debranched chickpea starch-LA complexes with broad chain length distributions.

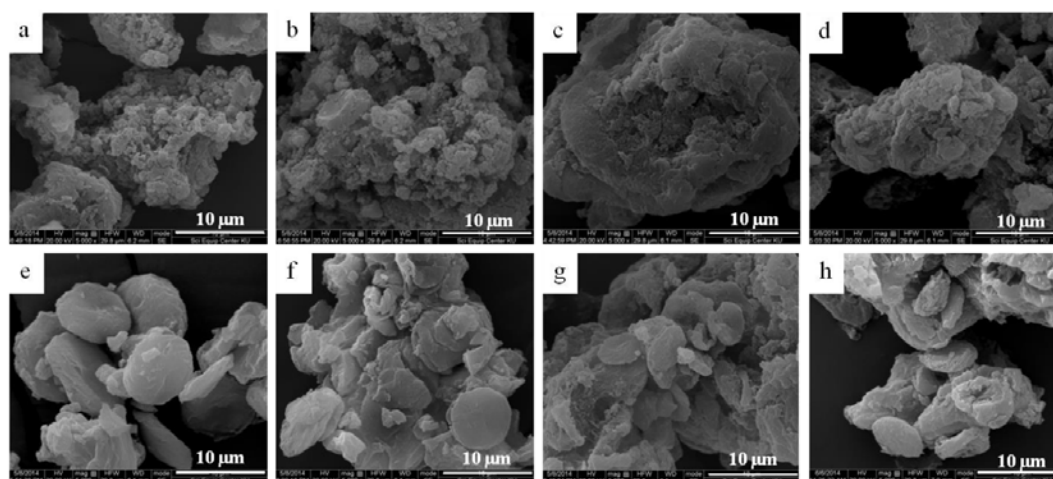


Figure 3. Scanning electron micrographs of debranched chickpea starch-LA complexes formed under different conditions: (a) 60°C_3%_1:0.1, (b) 60°C_3%_1:1, (c) 60°C_10%_1:0.1, (d) 60°C_10%_1:1, (e) 95°C_3%_1:0.1, (f) 95°C_3%_1:1, (g) 95°C_10%_1:0.1 and (h) 95°C_10%_1:1. Scale bar represent 10 mm.

Table 2. Relative crystallinity (RC, %) of the individual major peaks, total RC, proportions of the crystal types (% of total RC) and crystal size of debranched chickpea starch-LA complexes.

Conditions	Relative crystallinity (%) of peaks identified in the angular range 4-36° (2θ)										V-type		B-type	Crystal size (nm)						
	5.6° 7.5° 10° 11.2°/ 13° 14.2° 15.1° 17° 17.8° 18.7° 19.9° 22°/ 23° 24° Total RC of RC of B-type										V-type	B-type								
													RC		B-type					
(11.6°)										[22.5°]										
60°C_C_3%_1:0.1	0.6	0.4	-	-	7.1	-	-	0.7	-	11.4	0.4	-	0.3	20.9 ^c	18.9 ^c	2.0 ^g	90 ^b	10 ^g	4.78 ^{de}	
60°C_C_3%_1:1	0.3	0.3	-	-	6.8	-	-	0.4	-	11.2	0.3	-	0.2	19.5 ^d	18.3 ^d	1.2 ^h	94 ^a	6 ^h	4.83 ^e	
60°C_C_10%_1:0.1	1.6	-	0.2	-	0.3	-	-	5.9	-	2.4	1.1	-	1.2	12.9 ^f	2.7 ^h	10.2 ^a	21 ^g	79 ^a	5.03 ^d	
60°C_C_10%_1:1	0.7	-	0.1	-	0.2	-	-	5.8	-	3.0	0.7	-	1.3	12.0 ^h	3.2 ^g	8.8 ^b	27 ^f	73 ^b	5.05 ^d	
95°C_C_3%_1:0.1	0.8	1.5	-	(1.6)	8.8	-	0.1	1.5	-	(1.8)	9.6	[1.8]	-	-	27.9 ^a	21.7 ^a	2.7 ^g	78 ^c	10 ^g	13.18 ^b
95°C_C_3%_1:1	0.7	1.2	-	(0.9)	8.7	-	0.2	1.8	-	(1.2)	7.4	[2.2]	-	-	24.7 ^b	19.5 ^b	3.1 ^g	79 ^c	13 ^e	14.31 ^a
95°C_C_10%_1:0.1	0.9	0.3	0.2	0.1	1.4	-	0.2	3.6	-	(0.3)	2.1	[2.0]	-	1.4	12.5 ^g	5.8 ^f	6.4 ^d	47 ^e	51 ^c	11.35 ^c
95°C_C_10%_1:1	1.5	0.5	0.2	0.2	2.4	-	0.3	3.5	-	(0.3)	3.5	[1.7]	-	1.4	15.9 ^e	8.1 ^e	7.5 ^e	51 ^d	47 ^d	11.46 ^c

The data in round brackets indicate additional shoulder-shaped peaks and the data in square brackets indicate an additional peak at $2\theta = 22.5^\circ$. Peaks at $2\theta = 7.5^\circ$, 13° , 19.9° and 22.5° were attributed to V_{at}-type polymorph; peaks at $2\theta = 5.6^\circ$, 10° , 11.2° , 14° , 15° , 17° , 22° and 24° were attributed to B-type polymorph; peaks at $2\theta = 5.6^\circ$, 10° , 11.2° , 15° , 17° , 17.8° and 23° were attributed to C-type polymorph.

* denotes C-type polymorph instead of B-type.

The crystal size of complexes was estimated from three main peaks corresponding to V_{at}-type pattern at $2\theta = 7.5^\circ$, 13° and 19.9° .

Values within a column followed by different letters are significantly different ($p < 0.05$).

Table 3. Complexed LA contents in debranched chickpea starch-LA complexes.

Conditions	Complexed lauric acid contents (g/100g dry sample)
60°C_3%_1:0.1	1.40 ^a
60°C_3%_1:1	1.48 ^a
60°C_10%_1:0.1	0.20 ^c
60°C_10%_1:1	0.22 ^c
95°C_3%_1:0.1	1.18 ^{ab}
95°C_3%_1:1	0.94 ^b
95°C_10%_1:0.1	0.34 ^c
95°C_10%_1:1	0.40 ^c

Values within a column followed by different letters are significantly different ($p < 0.05$).

3.4 Thermostability of Complexes

Three or four separate endotherms were observed when heating debranched chickpea starch-LA complexes by DSC, depending on the sample (Table 4). The first endothermic peak at temperatures between 47.2 and 69.8°C was present in all samples, and was attributed to the melting of non-complex retrograded amylopectin short chains [27]. The enthalpies of retrogradation were related to the quantity of B- or C-type crystallites observed by XRD. The low temperature transition was not caused by melting of uncomplexed LA because DSC analysis of the free LA observed by several studies reported that melting occurred around 39.2-52.3°C [11]. According to Gidley and Bulpin [28], the minimum chain length required to form retrograded starch double helices is 10 anhydroglucose units (AGU). The low Mw linear chains (fraction with DP <10) were therefore too short to form the stable double helices and remained in the solution, and were discarded during the washing of the samples. Putseys et al. [20] suggested that theoretically 18 glucose units are required to complex one lipid molecule with more than 14 carbon atoms, forming a helix with three turns (6 AGU per turn). Godet et al. [10] suggested that the

critical chain length required to accommodate two LA molecules (12 carbon atoms per molecule) for complexation is 20-30 glucose residues. Therefore, the debranched starch chains that could retrograde and precipitate without being washed away and without forming a complex were probably in the range 10-17 AGU. A large proportion of glucan chains from debranched chickpea starch belonged to this fraction (10-17 AGU) (Table 1 in section 2.3), which explains the significant amount of retrograded chains and the large enthalpies of the first endothermic peak observed by DSC.

The second and the third endothermic peaks at temperatures in the range 86.7-102.8°C and 103.9-122.9°C respectively, were attributed to the dissociation of less ordered type I and semicrystalline type II starch-LA complexes, respectively [20]. Type I complexes were predominantly obtained at 60°C, which favored nucleation. Type II complexes were formed at 95°C, and were more thermostable than type I counterparts, by allowing sufficient propagation and resulting in structures with well-defined and larger crystalline regions [7].

The peak dissociation temperature of complexes was in the range 92.3-117°C.

Complexes formed at higher temperature (95°C) and lower starch and LA concentrations tended to have higher peak dissociation temperatures, which may indicate better stability and perfection (size homogeneity) of crystallite complexes under these conditions.

In addition, a bimodal melting of type II complexes at peak temperatures 111.2°C and 117.0°C was observed with complexes formed at 95°C, 3% starch concentration and 1:0.1 starch/LA mole ratio (Figure 4). The bimodal melting indicated that two subgroups of type II crystalline complexes with different heat stabilities were formed: type IIa and type IIb [29]. This phenomenon has been ascribed to the annealing kinetic of type IIa complexes

during the DSC measurement: partial melting of type IIa, recrystallization into type IIb, followed by final melting of type IIb complexes. The dissociation enthalpies of type I and type II complexes, especially the predominant type, were positively correlated with the amounts of complexed LA observed by GC ($R^2 = 0.94$).

A fourth endothermic peak in temperature range 137-160°C was present in all samples, and associated with the melting of retrograded amylose from uncomplexed amylose chains [30]. These endotherms were rather disorganized (irregular shape) and their enthalpies seemed inversely related to the enthalpies of retrogradation of B- and C-type crystallites.

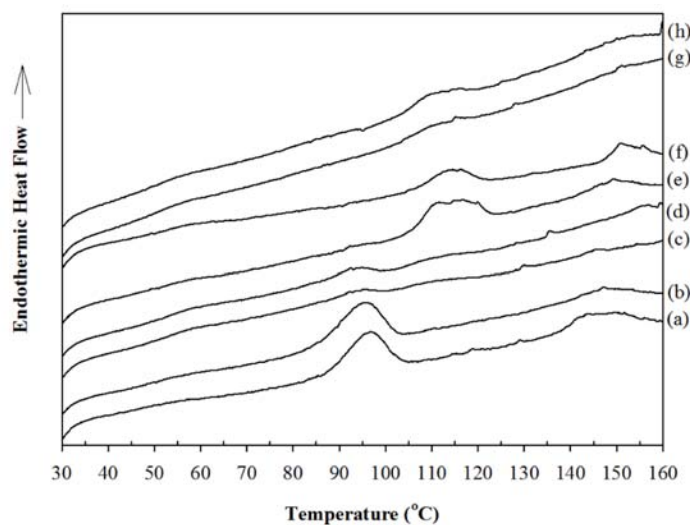


Figure 4. DSC thermograms of debranched chickpea starch-LA complexes formed under different conditions: (a) 60°C_3%_1:0.1, (b) 60°C_3%_1:1, (c) 60°C_10%_1:0.1, (d) 60°C_10%_1:1, (e) 95°C_3%_1:0.1, (f) 95°C_3%_1:1, (g) 95°C_10%_1:0.1 and (h) 95°C_10%_1:1.

Table 4. Thermal properties of debranched chickpea starch-LA complexes.

Conditions	Peak I				Peak II				Peak III				Peak IV			
	To (°C)	Tp (°C)	Tc (°C)	ΔH (J/g)	To (°C)	Tp (°C)	Tc (°C)	ΔH (J/g)	To (°C)	Tp (°C)	Tc (°C)	ΔH (J/g)	To (°C)	Tp (°C)	Tc (°C)	ΔH (J/g)
60°C_3%_1:0.1	47.18	53.67	63.26	0.96 ^b	87.13	96.00	102.77	8.69 ^b	-	-	-	-	136.97	146.83	156.81	3.00 ^b
60°C_3%_1:1	47.61	54.83	64.91	0.91 ^b	86.85	95.67	102.24	9.63 ^a	-	-	-	-	138.27	147.17	156.98	3.43 ^a
60°C_10%_1:0.1	48.16	58.33	69.70	1.40 ^a	88.01	93.67	99.25	1.41 ^d	103.91	110.83	120.61	0.53 ^c	141.40	152.33	159.55	1.12 ^f
60°C_10%_1:1	47.83	58.17	69.77	1.25 ^{ab}	86.70	92.33	97.85	1.86 ^c	105.02	109.67	118.40	0.64 ^c	146.31	153.50	159.60	0.83 ^f
95°C_3%_1:0.1	47.92	58.33	67.44	1.06 ^{ab}	91.79	92.50	97.90	0.29 ^e	105.73	111.17	122.88	6.86 ^a	146.27	149.17	157.48	2.69 ^c
95°C_3%_1:1	48.16	57.67	66.34	1.18 ^{ab}	-	-	-	-	106.74	114.33	121.29	3.93 ^b	147.69	150.83	159.29	2.30 ^d
95°C_10%_1:0.1	47.45	56.83	66.15	1.40 ^a	-	-	-	-	105.09	110.00	120.00	2.05 ^d	149.00	151.00	159.71	1.83 ^e
95°C_10%_1:1	48.72	56.00	66.28	1.22 ^{ab}	-	-	-	-	104.79	109.83	119.74	3.38 ^c	141.70	150.00	156.23	1.98 ^e

Values within a column followed by different letters are significantly different ($p < 0.05$).

4. CONCLUSIONS

Forming debranched chickpea starch-LA complexes is a competitive process with retrogradation, as the two phenomena take place under similar conditions of temperature and over similar timescales (hours). Higher temperature (95°C) resulted in higher total RC, both from complexes and retrograded

starch. The proportion of V-type crystallites (complexes) and B- or C-type crystallites (retrograded starch chains) depended on temperature and starch concentration: Overall the formation of V-type crystallites was dominant, however at 95°C the proportion of retrograded starch was higher compared to 60°C. Lower starch concentration favored

the formation of debranched chickpea starch-LA complexes, while crystallite size, morphology and dissociation temperature of complexes were affected by the complexation temperature. At 60°C, the formation of smaller crystallites was favored, while at 95°C torus/disc spherulites were obtained. The change in starch/LA mole ratio from 1:0.1 to 1:1 had a limited influence on the formation of complexes. The reaction conditions 3% w/w starch concentration and 60°C gave the highest complexation, but with lower thermostability and smaller crystallite sizes compared to the complexation at 95°C, which gave highly crystalline torus/disc spherulites. The differences in complexation, crystalline structure, morphology and thermostability among debranched chickpea starch-LA complexes suggest that combining debranching pretreatment with controlled complexation conditions can be used to design complexes with tailored properties, morphology (spherulites), crystallite size, and thermostability (type I, IIa, IIb). Such complexes can find applications as ingredients in the food industry, for instance to encapsulate sensitive compounds.

ACKNOWLEDGEMENTS

This research was financially supported by the Thailand Research Fund (TRF) through the Royal Golden Jubilee (RGJ) Ph.D. Program (Grant No. PHD/0254/2551). The authors are grateful to Dr. Kittiwut Kasemwong, National Nanotechnology Center, for the XRD instrument. We appreciate Mr. Suparoek Henpraserttae, National Metal and Materials Technology Center, for the XRD calculation guidance and Dr. Véronique Perrier, Montpellier SupAgro, for the GC instrument.

REFERENCES

- [1] Immel S. and Lichtenthaler F.W., *Starch/Stärke*, 2000; **52**: 1-8.
- [2] Conde-Petit B., Escher F. and Nuessli J., *Trends Food Sci. Technol.*, 2006; **17**: 227-235.
- [3] Lay Ma U.V., Floros J.D. and Zeigler G.R., *Carbohydr. Polym.*, 2011; **83**: 1869-1878.
- [4] Hasjim J., Lee S.O., Hendrich S., Setiawan S., Ai Y. and Jane J.L., *Cereal Chem.*, 2010; **87**: 257-262.
- [5] D'Silva T.V., Taylor J.R.N. and Emmambux M.N., *J. Cereal Sci.*, 2011; **53**: 192-197.
- [6] Biais B., Le Bail P., Robert P., Pontoire B. and Buléon A., *Carbohydr. Polym.*, 2006; **66**: 306-315.
- [7] Biliaderis C.G. and Galloway G., *Carbohydr. Res.*, 1989; **189**: 31-48.
- [8] Fanta G.F., Felker F.C., Shogren R.L., Byars J.A. and Salch J.H., *Carbohydr. Polym.*, 2005; **61**: 222-230.
- [9] Fanta G.F., Felker F.C., Shogren R.L. and Salch J.H., *Carbohydr. Polym.*, 2008; **71**: 253-262.
- [10] Godet M.C., Bizot H. and Buléon A., *Carbohydr. Polym.*, 1995; **27**: 47-52.
- [11] Zhang B., Huang Q., Luo F.X. and Fu X., *Food Hydrocoll.*, 2012; **28**: 174-181.
- [12] Yotsawimonwat S., Siroth K., Kaewvichit S., Piyachomkwan K., Jane J.L. and Sirithunyalug J., *Int. J. Biol. Macromol.*, 2008; **43**: 94-99.
- [13] Hilmarsson H., Traustason B.S., Kristmundsdottir T. and Thormar H., *Arch. Virol.*, 2007; **152**: 2225-2236.
- [14] Hood L.F. and Mercier C., *Carbohydr. Res.*, 1978; **61**: 53-66.

- [15] Kiatponglaarp W., Tongta S., Rolland-Sebaté A. and Buléon A., *Carbohydr. Polym.*, 2015; **122**: 108-114.
- [16] Bertoft E., *Carbohydr. Polym.*, 2004; **57**: 211-224.
- [17] Lopez-Rubio A., Flanagan B.M., Gilbert E.P. and Gidley M.J., *Biopolymers*, 2008; **89**: 761-768.
- [18] Hizukuri S. and Nikuni J., *Nature*, 1957; **180**: 436-437.
- [19] Rappenecker G. and Zugenmaier P., *Carbohydr. Res.*, 1981; **89**: 11-19.
- [20] Putseys J.A., Lamberts L. and Delcour J.A., *J. Cereal Sci.*, 2010; **51**: 238-247.
- [21] Cai L. and Shi Y.C., *Carbohydr. Polym.*, 2014; **105**: 341-350.
- [22] Kim J.Y. and Lim S.T., *Carbohydr. Polym.*, 2009; **76**: 110-116.
- [23] Hoover R. and Ratnayake W.S., *Food Chem.*, 2002; **78**: 489-498.
- [24] Tang M.C. and Copeland L., *Carbohydr. Polym.*, 2007; **67**: 80-85.
- [25] Le Bail P., Buléon A., Shiftan D. and Marchessault R.H., *Carbohydr. Polym.*, 2000; **43**: 317-326.
- [26] Kalinka G. and Hinrichsen G., *Acta Polym.*, 1997; **48**: 256-261.
- [27] Noda T., Takahata Y., Sato I., Morishita T., Ishiguro K. and Yamakawa O., *Carbohydr. Polym.*, 1998; **37**: 153-158.
- [28] Gidley M.J. and Bulpin P.V., *Carbohydr. Polym.*, 1987; **161**: 291-300.
- [29] Biliaderis C.G. and Seneviratne H.D., *Carbohydr. Polym.*, 1990; **13**: 185-206.
- [30] Biliaderis C.G., Page C.M., Slade L. and Sirett R.R., *Carbohydr. Polym.*, 1985; **5**: 367-389.